Fuel 288 (2021) 119667

Contents lists available at ScienceDirect

Fuel

journal homepage: www.elsevier.com/locate/fuel

Full Length Article

Skeletal and reduced kinetic models for methane oxidation under engine-relevant conditions

Jingyi Su [a], Yunchao Wu [b], Yiqing Wang [a], Xinyi Chen [a], Zheng Chen [a,*]

[a] Skltcs, Capt, Bic-ESAT, College of Engineering, Peking University, Beijing 100871, China
[b] Convergent Science Inc., 6400 Enterprise Lane, Madison, WI 53719, USA

ARTICLE INFO

Keywords:
Methane oxidation
Kinetic model reduction
Ignition
Flame propagation
Engine-relevant condition

ABSTRACT

Natural gas is a promising alternative fuel which can be used in internal combustion engines to reduce carbon emission. Therefore the combustion properties of methane, the major component of natural gas, have received great attention recently. This work aims to provide skeletal and reduced kinetic models for methane oxidation, which can be used for efficient simulations of methane combustion under engine-relevant conditions. The Foundational Fuel Chemistry Model (FFCM-1) developed at Stanford University served as the starting kinetic model for the reduction process. A 25 species skeletal model was firstly obtained by using sensitivity analysis and a 17 species reduced model was subsequently obtained through quasi-steady-state assumptions. The reduction procedure was performed within the parameter range of pressure from 1 to 120 atm, initial temperature for homogeneous ignition from 1000 to 2500 K, and equivalence ratio from 0.6 to 1.4, which includes the engine relevant conditions. Extensive validations of the present skeletal and reduced kinetic models were demonstrated through comparison with the original FFCM-1 model in the prediction of the homogeneous ignition, extinction and ignition in perfectly stirred reactor, premixed flame propagation and detonation properties. Very good agreement is achieved and thereby the original FFCM-1 model can be replaced by the present skeletal or reduced kinetic models in simulations of methane combustion.

1. Introduction

Natural gas is one of the promising alternative fuels which can be used in spark-ignition and compression-ignition engines [1]. Methane is the major component of natural gas and it has similar combustion properties as natural gas. Therefore, methane's combustion properties under engine-relevant conditions have received great attention recently (e.g., [1–4]).

Numerical simulation is currently one of the most important research tools for understanding fundamental combustion processes and it can be used in the development of high-performance natural gas engines [5,6]. To achieve quantitative prediction, multi-step or even detailed kinetic model instead of simplified one- or two-step chemistry should be applied in the numerical simulations [6,7]. However, applying the detailed kinetic model in the simulation can be time consuming due to the large number of species and the severe chemical stiffness. To achieve efficient combustion simulation, the detailed kinetic model needs to be adequately reduced before it is used in simulation. In the recent decades, mechanism reduction methods have been extensively studied [7,8]. The first category of reduction methods is the skeletal reduction, which quantifies the importance of the species and then eliminates unimportant species and reactions from the detailed mechanism. These methods include sensitivity analysis [9], principal component analysis [10], directed relation graph (DRG) [11–13], DRG with error propagation (DRGEP) [14], path flux analysis (PFA) [15], global pathway selection (GPS) [16], and Linearized error propagation (LEP) [17], etc. Another category is the time scale analysis, which assumes the fast processes decay in a transient time. The representative methods include quasi-steady-state approximations (QSSA) [18], partial equilibrium assumptions (PEA) [19] and intrinsic low-dimensional manifold (ILDM) [20], etc.

The objective of this work is to provide compact skeletal and reduced kinetic models for methane oxidation, which can be applied in efficient methane combustion simulations especially under engine-relevant conditions. Though in the literature there are several skeletal or reduced kinetic models for methane oxidation (e.g., [21,22]), most of them were based on the GRI mechanism which are suitable for flame propagation at high pressures [3]. In the following, first the performance

* Corresponding author.
E-mail address: cz@pku.edu.cn (Z. Chen).

https://doi.org/10.1016/j.fuel.2020.119667
Received 31 August 2020; Received in revised form 28 October 2020; Accepted 1 November 2020
Available online 15 November 2020

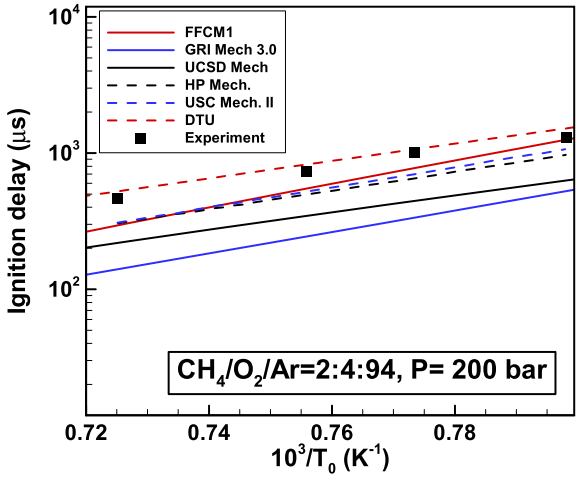

Fig. 1. Experimental and computed ignition delay time of stoichiometric CH_4/O_2/Ar mixtures at 200 bar, $T_0 = 1253 \sim 1379$ K. The experimental data, results of HP Mech. and USC Mech. II are from Karimi et al. [29].

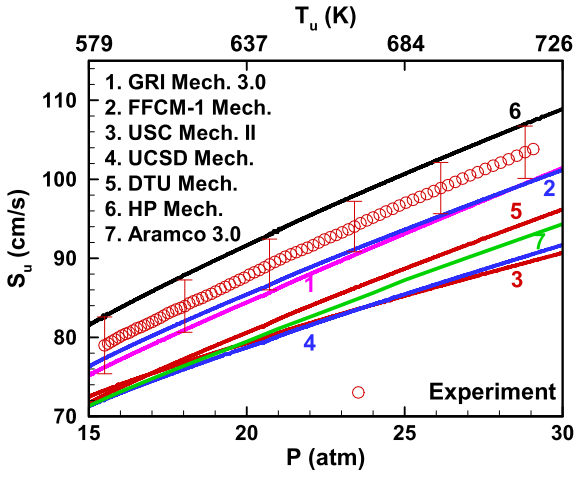

Fig. 2. Experimental measured and computed laminar flame speeds for the stoichiometric mixture ($1.0CH_4 + 2.0O_2 + 1.214\ N_2 + 10.926He$) along the P-T_u isentrope with the initial pressure and temperature of $P_0 = 6$ atm, $T_{u,0} = 424$ K. The experimental data are from Wang et al. [3].

of different kinetic models in terms of predicting methane combustion under engine-relevant conditions is described. Due to the accuracy compared with other kinetic models, the Foundational Fuel Chemistry Model (FFCM-1, for which the skeletal/reduced models do not exist in the literature) [23] is selected as the starting kinetic model for the mechanism reduction process. After that, the reduction process is introduced and the skeletal and reduced kinetic models are obtained. Lastly, extensive validations of the obtained skeletal and reduced kinetic models against the original FFCM-1 model in the prediction of the homogeneous ignition process, extinction and ignition in perfectly stirred reactor (PSR), premixed flame propagation and detonation properties are performed.

2. Methodologies

2.1. The starting kinetic model for methane

Due to the simple structure and widely application of methane, its oxidation kinetic has been studied by different research groups. A widely used methane mechanism is GRI Mech 3.0 which consists of 53 species and 325 reactions [24]. GRI Mech 3.0 is an optimized model and it includes the NOx sub chemistry. Other available kinetic models for methane combustion include USC Mech II [25], UCSD Mech [26], HP Mech [27] and DTU Mech [28]. Recently, the FFCM-1 model, consisting of 38 species and 291 reactions, has been developed by the collaboration research between Stanford University and SRI International [23]. The FFCM-1 model was optimized by a comprehensive uncertainty quantification analysis against a target set of fundamental combustion dataset over a wide range of conditions and phenomena.

Among these kinetic models mentioned above, the FFCM-1 model has been demonstrated to be able to predict methane combustion accurately under engine-relevant conditions. Using a high pressure shock tube, Karimi et al. [29] measured methane autoignition delays in carbon dioxide and argon diluents at pressure of 100 and 200 bars. Fig. 1 compares the experimental data with the predictions from different kinetic models. It is seen that the FFCM-1 model can accurately predict the autoignition delay of methane at high pressure up to 200 bar.

Wang et al. [3] assessed the performance of different kinetic models in terms of predicting the laminar flame speeds (LFSs) of methane/air under engine-relevant conditions. Experiments for spherically expanding flames were conducted to measure the LFSs of a $CH_4/O_2/N_2$/He mixture under a broad range of pressures and temperatures (15–30 atm, 405–514 K and 579–726 K) [3]. As shown in Fig. 2, the FFCM-1 model closely predicts the laminar flame speeds at high pressures and temperatures.

The above results show that the FFCM-1 model is the most accurate in predicting the ignition and flame propagation for methane under engine-relevant conditions. Therefore, the FFCM-1 model was selected as the starting kinetic model in generating the compact kinetic models.

It is noted that a 19-species reduced kinetic model has been developed based on GRI Mech 3.0 by Lu and Law [21]. However GRI Mech 3.0 was shown to greatly over-predict and under-predict the laminar flame speed and ignition delay, receptively, for methane/air at high pressures [3,29]. This is due to the fact that the pressure dependence of the reaction rate for H + O2 + M = HO2 + M is not adequately considered in GRI Mech 3.0, and that GRI Mech 3.0 does not consider methylperoxy (CH_3O_2) and methyl peroxide (CH_3O_2H) which are vital to the oxidation of methane at high pressures [30]. Therefore, the 19-species reduced kinetic model of GRI 3.0 is not suitable under engine-relevant conditions.

2.2. Methodology for kinetic model reduction

To obtain compact models suitable for engine applications, the reduction was performed within the parameter range of pressure from 1 to 120 atm, initial temperature for ignition problems from 1000 to 2500 K, and equivalence ratio from 0.6 to 1.4, focusing on the high-temperature and high-pressure conditions.

Since the detailed mechanism only contains 38 species, the brute force sensitivity analysis [31] was directly employed to achieve maximum reduction. Note the brute force sensitivity analysis is time consuming since it directly measures the reduction error through comparing the target flame features before and after reduction, therefore it usually applied in reducing relatively small mechanisms, for example in the present condition. The target parameters used in the sensitivity analysis included auto-ignition delay time under constant pressure condition and extinction residence time in PSR, since previous research indicates that that skeletal mechanisms derived from auto-ignition and PSR in most cases can be readily extended to more complex systems [7]. This is because reaction states sampled from auto-ignition carry the information on important reaction pathways controlling ignition, while those from PSR carry the information on reactions controlling flame extinction and high temperature flame chemistry. To achieve a relatively high accurate skeletal model, an error tolerance of 0.2 was used and a skeletal mechanism with 25 species and 145 reactions was obtained. The worst-case errors for the ignition delay time and extinction residence time for the reduction range are 0.17 and

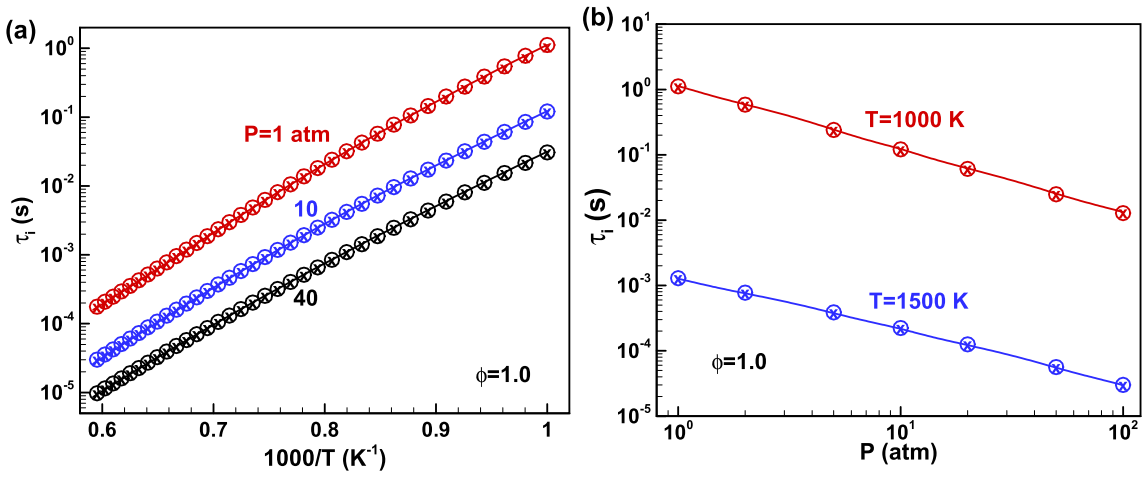

Fig. 3. Change of the ignition delay time with the (a) initial temperature and (b) initial pressure for a stoichiometric CH_4/air mixture predicted by the detailed (solid lines), skeletal (open circles) and reduced (crosses 'x') kinetic models.

0.15 respectively.

The skeletal kinetic model was further reduced through quasi-steady-state (QSS) assumptions to obtain the reduced kinetic model. Eight QSS species including CH, CH_2, HCO, CH_2OH, CH_3O, C_2H_3, C_2H_5, and CH_2CHO were identified by a systematic method based on the computational singular perturbation (CSP) [21], inducing a final 17-species reduced kinetic model. The reaction rates for the reduced kinetic model were evaluated through a systematically generated subroutine, in which the reaction rate coefficients are evaluated using the efficient transformed form as described in work of Lu et al. [7]. In addition, the concentrations of QSS species were obtained through the linearized quasi steady state approximations solved with a quasi-steady state graph method (LQSSA-QSSG) [32]. Both the skeletal and reduced kinetic models are provided in the Supplementary Documents.

3. Model validation

To validate the present skeletal and reduced kinetic models, the homogeneous ignition, extinction and ignition in perfectly stirred reactor, premixed flame propagation and detonation properties were compared with the detailed FFCM-1 model.

3.1. Homogeneous autoignition

Ignition delay is one of the most important targets for kinetic model development and reduction. Therefore, the zero-dimensional homogeneous ignition process under constant pressure was considered and simulated using SENKIN [33]. The ignition delay times, τ_i, defined as the time for the occurrence of maximum temperature rise rate, for methane/air mixture are calculated using the original FFCM-1 model and the skeletal and reduced models over a broad range of pressure, temperature and equivalence ratio. Stoichiometric mixture results at different pressures and temperatures are compared in Fig. 3.

Fig. 3(a) shows that the ignition delay time increases exponentially with the inverse of the initial temperature. Fig. 3(b) reveals that the ignition delay time is nearly proportional to the inverse of the pressure. These trends are consistent with the homogeneous ignition theory. It is seen the results predicted by skeletal and reduced models closely agree with those by the detailed mechanism, with a maximum relative difference of 5.3%. For off-stoichiometric mixtures similar results were obtained and were not shown here.

Besides the ignition delay time τ_i, another important parameter characterizing the ignition process is the excitation time τ_e, which represents the duration of heat release and is usually several order smaller than the ignition delay time. The excitation time, defined by the period between 5% and the peak heat release rate, is important for detonation

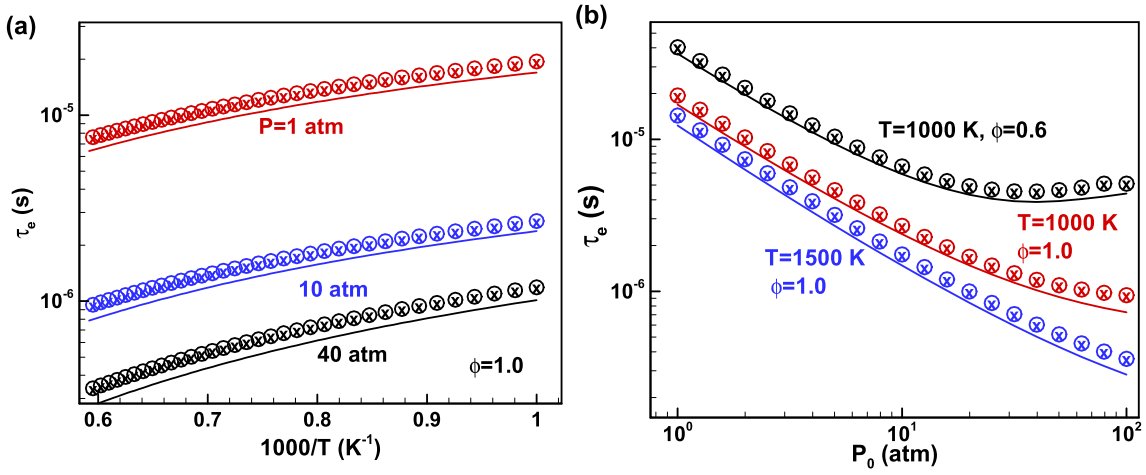

Fig. 4. Change of the excitation time with the (a) initial temperature and (b) initial pressure for a CH_4/air mixture predicted by the detailed (solid lines), skeletal (open circles) and reduced (crosses 'x') kinetic models.

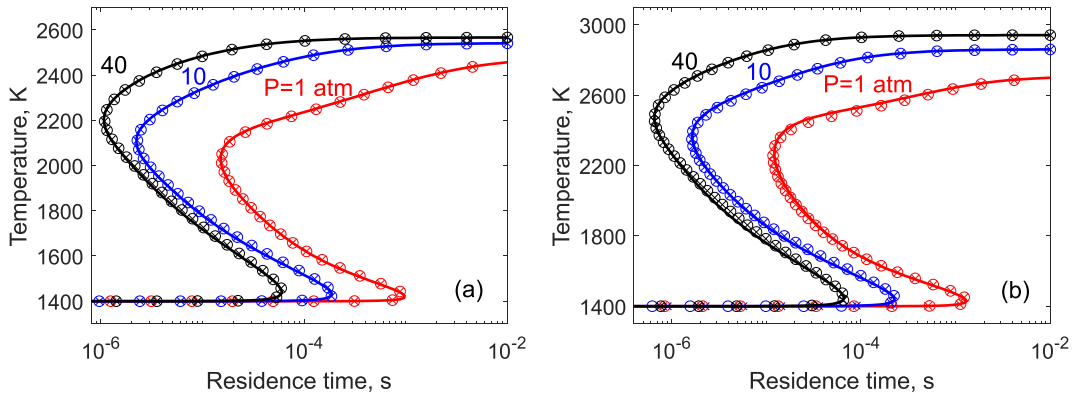

Fig. 5. The S-curves for PSR with an inlet temperature of 1400 K for CH_4/air with (a) $\phi = 0.6$ and (b) $\phi = 1.0$. The results are from the detailed (solid lines), skeletal (open circles) and reduced (crosses 'x') kinetic models.

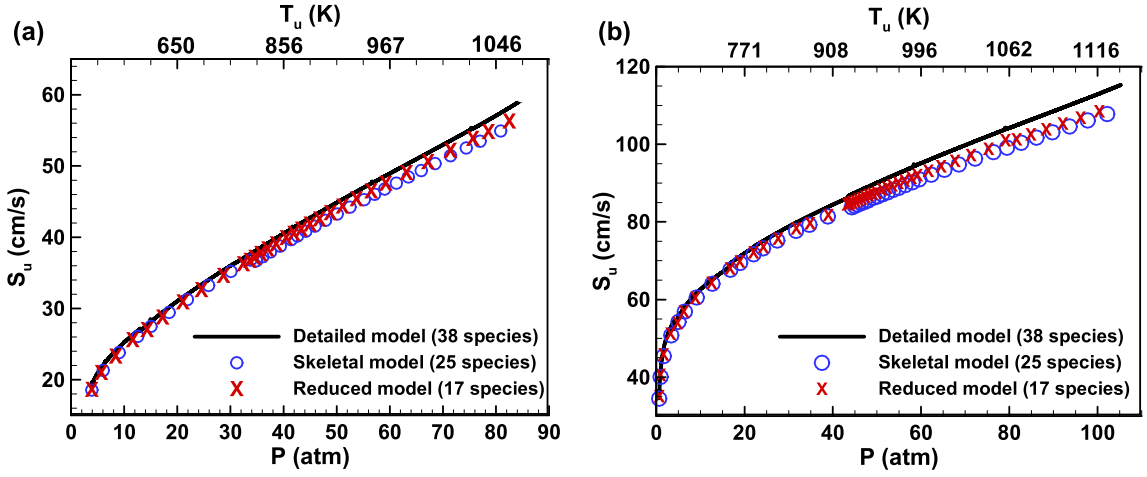

Fig. 6. Laminar flame speeds of (a) fuel-lean ($\phi = 0.6$) and (b) stoichiometric ($\phi = 1$) CH_4/air mixtures predicted by the detailed, skeletal and reduced kinetic models. The unburned gas pressure and temperature, (P, T_u), satisfy the isentropic compression relationship with ($P_0 = 1$ atm, $T_{u,0} = 298$ K).

development from temperature gradient [34–36]. Fig. 4 compares the excitation time predicted by the detailed, skeletal and reduced kinetic models for different pressures, temperatures, and equivalence ratios. It is seen that the reduced and skeletal models agree well with the detailed model with slightly overestimate. Note that similar results for fuel lean mixture have also be obtained but not shown in Fig. 4 due to the overlapping of the results for different equivalence ratios.

The above results indicate that the skeletal and reduced kinetic models can accurately predict the ignition process and thereby can replace the detailed FFCM-1 model. It is noted that the maximum difference between the results from the skeletal and reduced kinetic models is within 1%, which implies the QSSA successfully reduces the number of species without reducing the accuracy.

3.2. PSR

The performance of the reduced and skeletal models in predicting the combustion in PSR is then examined. Fig. 5 displays PSR *S*-curves for pressures of 1, 10 and 40 atm under stoichiometric and lean conditions. The *S*-curves predicted by the skeletal and reduced kinetic models are shown to overlap with the one by the detailed model, demonstrating that the skeletal and reduced kinetic models can accurately predict the ignition and extinction processes in PSR.

3.3. Premixed flames

Laminar flame speed (LFS) is another important target for kinetic model development and reduction [37]. To further validate the skeletal and reduced kinetic models, the LFSs of CH_4/air mixtures at normal and elevated temperatures and pressures were calculated using the constant-volume spherically expanding flame (CVSEF) method (see [38] and references therein). In this method, LFS as a function of initial temperature/pressure can be obtained after running the code for one specific case [38]. This method is much more efficient than using CHEMKIN-PREMIX or Cantera. Besides, CVSEF has the advantage of obtaining the LFSs at very high temperatures and pressures close to or under engine-relevant conditions. Therefore, this method was recommended by Faghih et al. [39] for assessing the performance of reduced kinetic models over a broad range of temperatures and pressures.

Fig. 6 plots the LFSs of lean and stoichiometric CH_4/air mixtures with the initial temperature and pressure up to 1000 K and 100 atm, respectively. Note that the unburned gas pressure increases with the unburned gas temperature following the isentropic compression relationship [39]. It is seen that the discrepancy among LFSs predicted by different kinetic models increases with unburned gas pressure. Nevertheless, the maximum difference is within 5%, indicating the skeletal and reduced kinetic models can accurately predict the LFSs of CH_4/air mixtures under engine-relevant conditions. It is noted that in experiments it is difficult to measure the LFSs at very high pressures and temperatures due to flame instability and autoignition in unburned gas.

The unsteady ignition kernel propagation is sensitive to kinetic models [40]. Therefore, the performance of the skeletal and reduced kinetic models in terms of predicting the ignition kernel and spherical flame propagation in a static stoichiometric CH_4/air mixture are

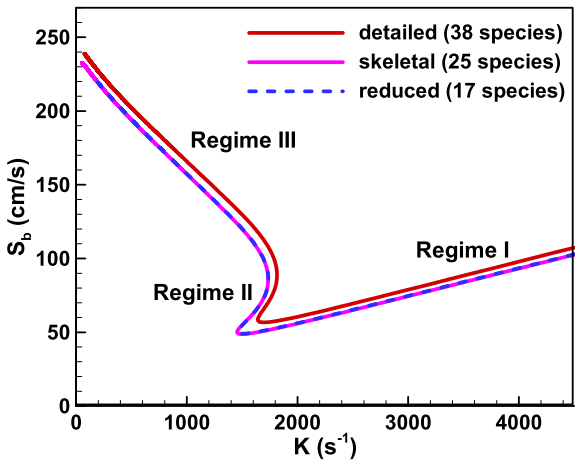

Fig. 7. Change of the spherical flame propagation speed with the stretch rate in a stoichiometric CH_4/air mixture at 300 K and 1 atm. The ignition energy is E_{ig} = 0.24 mJ and different lines represent results predicted by the detailed, skeletal and reduced kinetic models.

assessed. The unsteady ignition and flame propagation process was simulated with the in-house code A-SURF [41,42] and the numerical model and specifications were similar to those in [43]. Fig. 7 shows that during the ignition kernel propagation there are three regimes: the ignition energy induced flame kernel propagation regime (I), the unsteady flame transition regime (II), and the normal flame propagation regime (III). Note that the over-driven flame propagation regime [43] does not appear since the effective Lewis number of the stoichiometric CH_4/air mixture is close to unity. It is observed that the different regimes were predicted by the skeletal and reduced kinetic models. Though there is slight under-prediction in the flame propagation speed, the overall agreement is satisfactory.

3.4. Detonation

Besides the autoignition and normal flame propagation, the detonation development and propagation, referred to as super-knock [44], might occur in internal combustion engines under certain conditions. Therefore, we also assessed the performance of the skeletal and reduced kinetic models in predicting the detonation properties.

First, we calculated the Chapman-Jouguet (CJ) speed, D_{CJ}, and the induction length, δ_{th}, of one-dimensional ZND detonation in CH_4/air mixtures using Cantera [45] and the results are shown in Fig. 8. It is seen that compared to the detailed model, the skeletal model can accurately predict the CJ speed and the induction length over a broad range of equivalence ratio. It is noted that the results from the reduced model was not obtained due to the lamination of Cantera in applying the QSS assumptions. Nevertheless, since almost the same results are predicted by

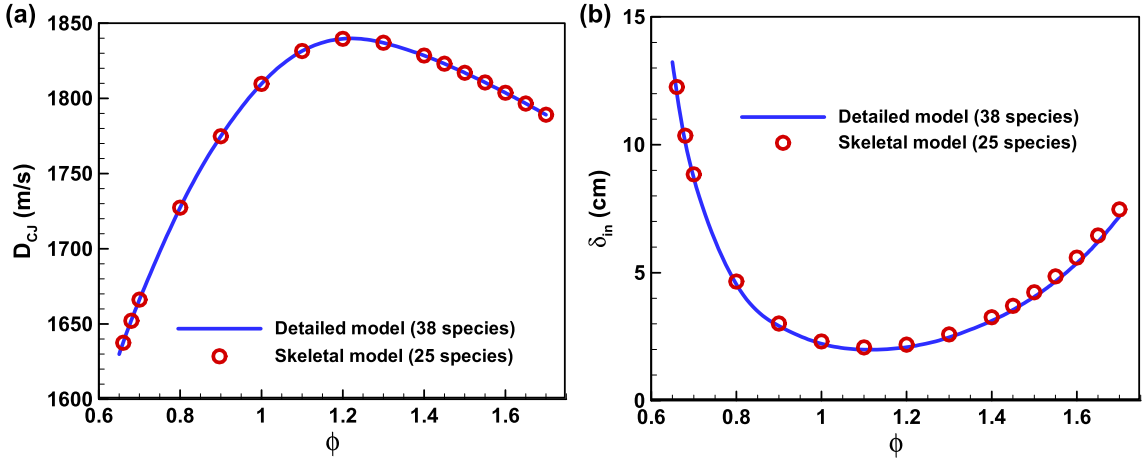

Fig. 8. (a) C-J detonation speed and (b) induction length of the steady ZND detonation structure for CH_4/air mixtures at 298 K and 1 atm.

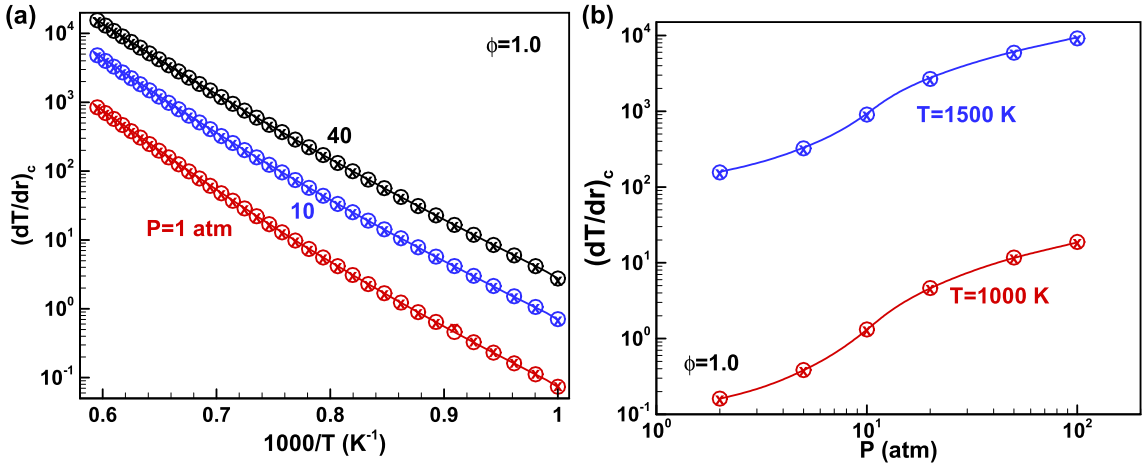

Fig. 9. Change of the critical temperature gradient with (a) the initial temperature and (b) the initial pressure for a stoichiometric CH_4/air mixture predicted by the detailed (solid lines), skeletal (open circles) and reduced (crosses 'x') kinetic models.

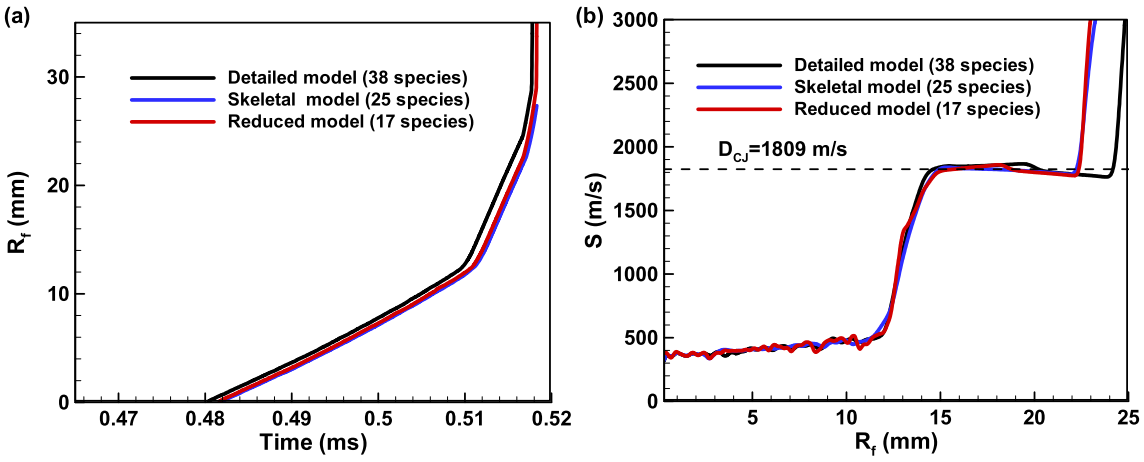

Fig. 10. Auto-ignitive reaction front propagation from a hot spot in a stoichiometric CH_4/air mixture initially at $T_0 = 1300$ K and $P_0 = 40$ atm. The hot spot has the temperature gradient of $(dT/dr)_0 = -1050$ K/m and radius of $r_0 = 11$ mm. (a) change of reaction front position R_f with time t; (b) change of reaction front propagation speed S with the position R_f.

the skeletal and reduced kinetic models in Figs. 3–7, the induction length predicted by these two models is expected to be also nearly the same. It is also noted that the FFCM-1 model has not be validated experimentally by characterized C-J detonation parameters.

Then, we considered the detonation development from temperature gradient [34–36,42,46]. The detonation development is determined by the coherent coupling between chemical reaction and pressure wave, and it occurs only when the reaction front speed, S, is in the same order as the sound speed, a. The following critical temperature gradient is defined for equivalent value of reaction front speed and sound speed [34]:

$$\left(\frac{dT_0}{dr}\right)_c = -\left(a\frac{d\tau_i}{dT_0}\right)^{-1} \quad (1)$$

The critical temperature gradient was widely used in studies on detonation development from a hot spot with linear temperature distribution [32–34,39,42]. Therefore, the critical temperature gradient predicted by the detailed, skeletal and reduced kinetic models are compared. The results in Fig. 9 show that very good consistency is achieved for a broad range of initial temperature and pressure with the worst case relative error within 2%.

We further simulated the detonation development from a hot spot using the detailed, skeletal and reduced kinetic models using the in-house code A-SURF [42,47,48]. In the simulation, a stoichiometric CH_4/air mixture initially at $T_0 = 1300$ K and $P_0 = 40$ atm was considered and the hot spot locates in the center has the initial temperature gradient of $(dT/dr)_0 = -1050$ K/m and radius of $r_0 = 11$ mm. More details of the specifications can be founded in our previous study [49]. It is shown in Fig. 10 that the auto-ignitive reaction front is initiated from the hot spot and it starts to propagate outwardly at around $t = 0.48$ ms. First, the reaction front propagates at the speed around 450 m/s. Then, the reaction front accelerates at around $t = 0.51$ ms, where the detonation develops and the propagation speed is around the CJ speed of $D_{CJ} = 1809$ m/s. Lastly, all the unburned gas auto-ignites at around $t = 0.517$ ms and the reaction front accelerates again. These observations are consistent with previous numerical results [34–36,42,46]. Fig. 10 shows that the detailed, skeletal and reduced kinetic models predict nearly the same position of detonation initiation and very close reaction front propagation speed, indicating the skeletal and reduced kinetic models can be used to replace the detailed model in simulations of detonation development from temperature gradient under engine-relevant conditions.

When an implicit solver like VODE is used in numerical integration, the computational time is proportional to n^r with n being the number of species and $r > 2$. Since the number of species in the detailed and reduced models is respectively 38 and 17, a speed-up factor of more than 5 can be achieved by using the reduced kinetic model compared with the detailed one.

4. Conclusions

Using the FFCM-1 model with 38 species as the starting kinetic model, we first obtained a skeletal kinetic model with 25 species through sensitivity analysis and then a reduced kinetic model with 17 species through quasi-steady-state assumptions. The present skeletal and reduced kinetic models were extensively validated by comparing the ignition delay and extinction time, ignition and extinction residence time in perfectly stirred reactor, laminar flame speed, ignition kernel propagation, CJ speed, detonation induction length, and detonation development predicted by the detailed and reduced kinetic models. Excellent agreements were observed for different pressures and temperatures under engine-related conditions. Therefore, the present skeletal or reduced kinetic models can be used to replace the detailed FFCM-1 model to achieve a speed up in the simulation. The present skeletal or reduced kinetic models are provided in the Supplementary Documents.

CRediT authorship contribution statement

Jingyi Su: Conceptualization, Methodology, Writing - review & editing, Methodology, Validation, Writing - original draft. **Yunchao Wu:** Methodology, Validation. **Yiqing Wang:** Methodology, Validation. **Xinyi Chen:** Methodology, Validation. **Zheng Chen:** Conceptualization, Methodology, Writing - review & editing.

Declaration of Competing Interest

The authors declare that they have no known competing financial interests or personal relationships that could have appeared to influence the work reported in this paper.

Acknowledgement

This work was supported by National Natural Science Foundation of China (Nos. 91841302 and 91741126). We thank Professor Tianfeng Lu at University of Connecticut for helpful discussion on kinetic model reduction.

Appendix A. Supplementary data

Supplementary data to this article can be found online at https://doi.org/10.1016/j.fuel.2020.119667.

References

[1] Korakianitis T, Namasivayam AM, Crookes RJ. Natural-gas fueled spark-ignition (SI) and compression-ignition (CI) engine performance and emissions. Prog Energy Combust Sci 2011;37(1):89–112. https://doi.org/10.1016/j.pecs.2010.04.002.

[2] Liberman M, Wang C, Qian C, Liu J. Influence of chemical kinetics on spontaneous waves and detonation initiation in highly reactive and low reactive mixtures. Combust Theor Model 2019;23(3):467–95. https://doi.org/10.1080/13647830.2018.1551578.

[3] Wang Y, Movaghar A, Wang Z, Liu Z, Sun W, Egolfopoulos FN, Chen Z. Laminar flame speeds of methane/air mixtures at engine conditions: performance of different kinetic models and power-law correlations. Combust Flame 2020;218:101–8. https://doi.org/10.1016/j.combustflame.2020.05.004.

[4] Huang J, Hill PG, Bushe WK, Munshi SR. Shock-tube study of methane ignition under engine-relevant conditions: experiments and modeling. Combust Flame 2004;136(1-2):25–42. https://doi.org/10.1016/j.combustflame.2003.09.002.

[5] Westbrook CK, Mizobuchi Y, Poinsot TJ, Smith PJ, Warnatz J. Computational combustion. Proc Combust Inst 2005;30(1):125–57. https://doi.org/10.1016/j.proci.2004.08.275.

[6] Chen JH. Petascale direct numerical simulation of turbulent combustion—fundamental insights towards predictive models. Proc Combust Inst 2011;33(1):99–123. https://doi.org/10.1016/j.proci.2010.09.012.

[7] Lu T, Law CK. Toward accommodating realistic fuel chemistry in large-scale computations. Prog Energy Combust Sci 2009;35(2):192–215. https://doi.org/10.1016/j.pecs.2008.10.002.

[8] Gou XL, Sun WT, Chen Z. Numerical methods for complicated chemical mechanism involved in combustion simulation. Sci Sin-Phys Mech Astron 2017;47(7):070006. https://doi.org/10.1360/SSPMA2016-00385.

[9] Turányi T. Sensitivity analysis of complex kinetic systems. Tools and applications. J Math Chem 1990;5(3):203–48.

[10] Vajda S, Valko P, Turányi T. Principal component analysis of kinetic models: principal component analysis of kinetic models. Int J Chem Kinet 1985;17(1):55–81. https://doi.org/10.1002/kin.550170107.

[11] Lu T, Law CK. A directed relation graph method for mechanism reduction. Proc Combust Inst 2005;30(1):1333–41. https://doi.org/10.1016/j.proci.2004.08.145.

[12] Lu T, Law CK. Linear time reduction of large kinetic mechanisms with directed relation graph: n-Heptane and iso-octane. Combust Flame 2006;144(1-2):24–36. https://doi.org/10.1016/j.combustflame.2005.02.015.

[13] Luo Z, Lu T, Maciaszek MJ, Som S, Longman DE. A reduced mechanism for high-temperature oxidation of biodiesel surrogates. Energy Fuels 2010;24(12):6283–93. https://doi.org/10.1021/ef1012227.

[14] Pepiotdesjardins P, Pitsch H. An efficient error-propagation-based reduction method for large chemical kinetic mechanisms. Combust Flame 2008;154(1-2):67–81. https://doi.org/10.1016/j.combustflame.2007.10.020.

[15] Sun W, Chen Z, Gou X, Ju Y. A path flux analysis method for the reduction of detailed chemical kinetic mechanisms. Combust Flame 2010;157(7):1298–307. https://doi.org/10.1016/j.combustflame.2010.03.006.

[16] Gao X, Yang S, Sun W. A global pathway selection algorithm for the reduction of detailed chemical kinetic mechanisms. Combust Flame 2016;167:238–47. https://doi.org/10.1016/j.combustflame.2016.02.007.

[17] Wu Y, Liu Y, Lu T. A linearized error propagation method for skeletal mechanism reduction. Combust Flame 2020;211:303–11. https://doi.org/10.1016/j.combustflame.2019.10.003.

[18] Peters N. Numerical and asymptotic analysis of systematically reduced reaction schemes for hydrocarbon flames. Lecture Notes in Physics. Berlin, Heidelberg: Springer; 1985. pp. 90–109.

[19] Smoke MD, Giovangigli V. Formulation of the premixed and nonpremixed test problems. Reduc Kinet Mech Asymptot Approx Methane-Air Flames 1991;384:1–28.

[20] Maas U, Pope SB. Simplifying chemical kinetics: intrinsic low-dimensional manifolds in composition space. Combust Flame 1992;88(3-4):239–64. https://doi.org/10.1016/0010-2180(92)90034-M.

[21] Lu T, Law CK. A criterion based on computational singular perturbation for the identification of quasi steady state species: a reduced mechanism for methane oxidation with NO chemistry. Combust Flame 2008;154(4):761–74.

[22] Chen Y, Chen JY. Towards improved automatic chemical kinetic model reduction regarding ignition delays and flame speeds. Combust Flame 2018;190:293–301.

[23] Smith G, Tao Y, Wang H. Foundational fuel chemistry model version 1.0 (FFCM-1); 2016. Available from: http://nanoenergy.stanford.edu/ffcm1.

[24] Smith G, Golden D, Frenklach M, Moriarty N, Eiteneer B, Goldenberg M, et al. GRI-Mech 3.0; 1999. Available from: http://combustion.berkeley.edu/gri-mech/version30/text30.html.

[25] Wang H, You X, Joshi A, Davis SG, Laskin A, Egolfopoulos F, et al. High-temperature combustion reaction model of H2/CO/C1–C4 compounds; 2007. Available from: http://www.ignis.usc.edu/USC_Mech_II.htm.

[26] Chemical-Kinetic Mechanisms for Combustion Applications; Available from: http://web.eng.ucsd.edu/mae/groups/combustion/mechanism.html.

[27] Shen X, Yang X, Santner J, Sun J, Ju Y. Experimental and kinetic studies of acetylene flames at elevated pressures. Proc Combust Inst 2015;35(1):721–8.

[28] Hashemi H, Christensen JM, Gersen S, Essen M, Levinsky H, Klippenstein S, et al. High-pressure oxidation of methane. Combust Flame 2016;172:349–64.

[29] Karimi M, Ochs B, Liu Z, Ranjan D, Sun W. Measurement of methane autoignition delays in carbon dioxide and argon diluents at high pressure conditions. Combust Flame 2019;204:304–19.

[30] Al. Tingas E, Manias DM, Sarathy SM, Goussis DA. CH4/air homogeneous autoignition: a comparison of two chemical kinetics mechanisms. Fuel 2018;223(JUL.1):74–85.

[31] Zheng XL, Lu TF, Law CK. Experimental counterflow ignition temperatures and reaction mechanisms of 1,3-butadiene. Proc Combust Inst 2007;31(1):367–75.

[32] Lu T, Law CK. Systematic approach to obtain analytic solutions of quasi steady state species in reduced mechanisms. J Phys Chem A 2006;110(49):13202–8.

[33] Lutz A, Kee R, Miller J. Senkin: a Fortran program for predicting homogeneous gas phase chemical kinetics with sensitivity analysis; 1991.

[34] Gu XJ, Emerson DR, Bradley D. Modes of reaction front propagation from hot spots. Combust Flame 2003;133(1/2):63–74.

[35] Dai P, Chen Z, Chen S, Ju Y. Numerical experiments on reaction front propagation in n-heptane/air mixture with temperature gradient. Proc Combust Inst 2015;35(3):3045–52.

[36] Gao Y, Dai P, Chen Z. Numerical studies on autoignition and detonation development from a hot spot in hydrogen/air mixtures. Combust Theory Model 2020;24:245–61.

[37] Chen Z. On the accuracy of laminar flame speeds measured from outwardly propagating spherical flames: methane/air at normal temperature and pressure. Combust Flame 2015;162(6):2442–53.

[38] Faghih M, Chen Z. The constant-volume propagating spherical flame method for laminar flame speed measurement. Sci Bull 2016;61:1–15.

[39] Mahdi F, Wang H, Zheng C. Effects of Soret diffusion on premixed flame propagation under engine-relevant conditions. Combust Flame 2018;194:175–9.

[40] Kim HH, Won SH, Santner J, Chen Z, Ju Y. Measurements of the critical initiation radius and unsteady propagation of n-decane/air premixed flames. Proc Combust Inst 2013;34(1):929–36.

[41] Chen Z. Effects of radiation and compression on propagating spherical flames of methane/air mixtures near the lean flammability limit. Combust Flame 2010;157(12):2267–76.

[42] Dai P, Chen Z. Supersonic reaction front propagation initiated by a hot spot in n-heptane/air mixture with multistage ignition. Combust Flame 2015;162(11):4183–93.

[43] Yuan W, Wang H, Zheng C. Effects of fuel stratification on ignition kernel development and minimum ignition energy of n-decane/air mixtures. Proc Combust Inst 2018;000:1–8.

[44] Wang Z, Liu H, Reitz RD. Knocking combustion in spark-ignition engines. Prog Energy Combust Sci 2017;61:78–112.

[45] Goodwin DG, Moffat HK, Speth RL. Cantera: an object-oriented software toolkit for chemical kinetics, thermodynamics, and transport processes. Version 2.3.0. Cantera Developers, Warrenville, IL; 2017.

[46] Dai P, Qi C, Chen Z. Effects of initial temperature on autoignition and detonation development in dimethyl ether/air mixtures with temperature gradient. Proc Combust Inst 2017;36(3):3643–50.

[47] Zheng C, Burke MP, Ju Y. Effects of Lewis number and ignition energy on the determination of laminar flame speed using propagating spherical flames. Proc Combust Inst 2009;32(1):1253–60.

[48] Chen Z. Effects of radiation and compression on propagating spherical flames of methane/air mixtures near the lean flammability limit. Combust Flame 2010;157:2267–76.

[49] Su J, Dai P, Chen Z. Detonation development from a hot spot in methane/air mixtures: effects of kinetic models. Int J Engine Res 2020;00:1–10.